Marine Pollution Bulletin 209 (2024) 117120

Contents lists available at ScienceDirect

Marine Pollution Bulletin

journal homepage: www.elsevier.com/locate/marpolbul

Application of concentration-weighted trajectory approach to identify sources with high anthropogenic mercury emissions in the East Asia

E.A. Lopatnikov *, M.V. Ivanov

V.I. Il'ichev Pacific Oceanological Institute, Far Eastern Branch Russian Academy of Science, 43, Baltiiskaya St., Vladivostok 690041, Russia

ARTICLE INFO

Keywords:
Gaseous elemental mercury
Source apportionment
Transboundary pollution
CWT analysis
East Asian seas

ABSTRACT

The study evaluates the applicability of the CWT method for identifying mercury sources in a region with high anthropogenic emissions. Analysis is conducted to compare results on grids of 1 × 1°, 0.5 × 0.5°, and 0.1 × 0.1°. New data on atmospheric atomic mercury concentrations over the Sea of Japan and the East China Sea are compared, with higher resolution enabling clearer source localization. Results show increased mercury concentrations in winter, likely due to the heating season, yet they remain lower than previous values. Comparing grid resolutions indicates higher resolution can better pinpoint sources and disregard some emissions. The analysis also confirms transboundary transfer of atomic mercury from northeast China to the southeast Korean Peninsula.

Mercury is a persistent and toxic chemical substance that can bioaccumulate and negatively affect human health (Chen et al., 2019; Fu et al., 2012). Particular attention focuses on atomic elemental mercury [GEM], which can enter the atmosphere and move in it for long distances over long periods, up to a year (AMAP/UNEP, 2013; Gustin et al., 2015). As a result of dry and wet deposition on the earth's surface, mercury can turn into methylmercury and have effects on human health and the ecosystem (Beckers and Rinklebe, 2017; Lindberg et al., 2007).

The following fact was proved 200 years ago. The increase in mercury concentration in the atmosphere is connected with the beginning of the industrial period (UNEP, 2013). The Asian Region is the largest contributor to atomic mercury emissions into the atmosphere (Pirrone et al., 2010). China is the leader (Zhang et al., 2015). The atmospheric transfer of GEM into the Sea of Japan from China and the Yellow Sea Region has previously been recorded many times (Kalinchuk et al., 2018, 2020). However, few studies focus on the winter period and the impact of the winter monsoon. The winter period shows increased GEM emissions into the atmosphere due to the burning of Hg-containing coal because of the beginning of the heating season (Pirrone et al., 2010; UNEP, U, 2013; Wang et al., 2000). The western part of the East China Sea and the Yellow Sea recorded GEM transfer from the Chinese mainland by the northern winter monsoon (Wang et al., 2017).

In recent years, the CWT approach has been widely used in studies on mercury monitoring in the atmosphere (Kalinchuk et al., 2020). It identifies potential regions-sources of mercury using inverse trajectories of air masses. Attempts to localize Hg(0) sources using CWT analysis from the Sea of Japan indicated an extensive source, extending from the east coast of China to the east coast of the Korean Peninsula (Kalinchuk et al., 2020).

The research purpose is to evaluate the applicability of the CWT analysis approach with the high resolution capability for the localization of the atomic mercury resources. The main research tasks are as follows:

To compare the CWT analysis approach of high resolution with low one.
To determine zones that suffer the influence of the transboundary transfer of the atomic mercury.
To analyze the specifics of the temporal and spatial spread of Hg(0) in the surface atmosphere of East Asian seas during the autumn and winter of 2019.
To assess the territorial contribution to mercury emissions into the surface atmosphere.

This paper uses the results of Hg(0) measures in the surface atmosphere of the Sea of Japan and the East China Sea. These measures were obtained in two stages during the 88th voyage of the Academic Lavrentyev R/V in October–December 2019. The passage from Port Vladivostok to the South China Sea and back (Fig. 1). Measures were conducted with the use of the atomic absorption analyzer for mercury RA-915 M (Lumex Ltd., Saint-Petersburg). The detection limit is 0.3 ng/

* Corresponding author.
E-mail address: lopatnikov@poi.dvo.ru (E.A. Lopatnikov).

https://doi.org/10.1016/j.marpolbul.2024.117120
Received 2 April 2024; Received in revised form 13 September 2024; Accepted 7 October 2024
Available online 15 October 2024

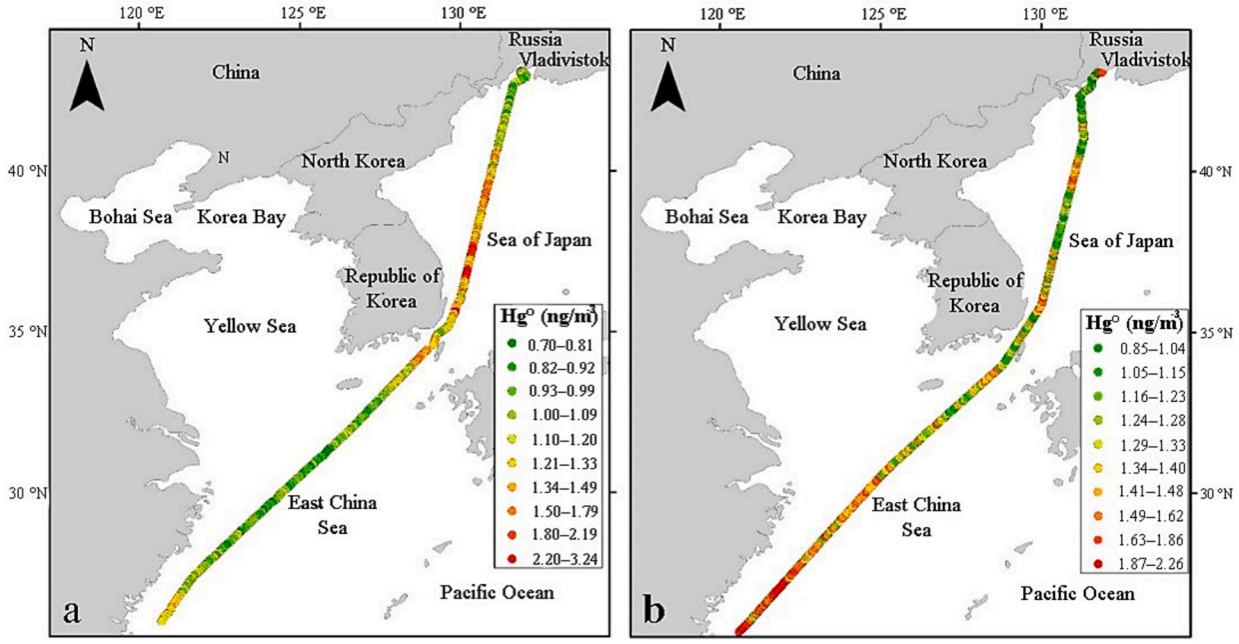

Fig. 1. Spatial distribution of Hg(0) in the surface atmosphere during the 88th voyage of the Academic Lavrentyev R/V from Vladivostok (a) and to Vladivostok (b), autumn-winter 2019.
Source: Compiled by the authors.

m^3 (Sholupov et al., 2004). The values were averaged in 1 min with a zero check every 5 min. In order to demonstrate the spatial and temporal distribution, the results were averaged at 30-minsute intervals. In order to perform the CWT analysis, the measures were averaged each hour of the study period. The main meteorological parameters were determined every 30 min with the use of weather station Davis Vantage Pro (Davis Instruments Corp., USA). These parameters include temperature, humidity, pressure, precipitation, solar radiation, wind speed, and direction.

In order to obtain return trajectories, the well-described HYSPLIT system with the GDAS1 meteorological database with ensemble option was used (Fang et al., 2018; Kalinchuk et al., 2020; Liu et al., 2019a), which allows obtaining 27 possible trajectories from a measuring point. The 72-hour reverse trajectories of the air masses were modeled for each hour of the researched period. Hence, 8.343 single trajectories were modeled.

In the CWT analysis, each inverse trajectory of air mass movement during the measurement is associated with the concentration of mercury (Hg(0)) obtained at that time (Kalinchuk et al., 2020). This study presents the results of an analysis with different grid cell sizes (i, j): the most widely used 0,5 × 0,5° (Liu et al., 2019b; Fang et al., 2018) and 1 × 1° (Kalinchuk et al., 2020), as well as in high resolution of 0,1 × 0,1° (Kalinchuk et al., 2022; Kalinchuk, 2023). In order to filter out emissions, only the CWTij values where at least two air mass trajectories intersected were considered.

To compare the potential sources of Hg(0), the entire territory of the region was plotted on a 0,1 × 0,1° grid. The percentage coverage of the area using CWT analysis was estimated by dividing the total number of cells in the region by the number of cells with a CWT value. The boundaries of the regions were used from open sources on the Internet, the boundaries of the regions of China (CASM et al., 1996).

During the study period, Mercury concentrations (ng/m^3) in the surface atmosphere varied from 0.69 to 3.2, average 1.25, median 1.21, and standard deviation 0.3. Hg(0) concentrations increased from the central part of the Sea of Japan to the Korean Strait along the vessel's voyage from the port of Vladivostok (Fig. 1a), reaching a maximum of 3.24 ng/m^3 near the eastern part of the Korean Peninsula. A decrease in concentration occurs as the vessel moves to Vladivostok (Fig. 1b). From southeast China to the central East China Sea, from 2.2 ng/m^3 to a median of 1.2 ng/m3. The average Hg(0) concentration in the surface atmosphere along the way from Vladivostok is 1.23 ng/m^3 for the Sea of Japan and 1.05 ng/m^3 for the East China Sea. During the way back, the values are 1.26 ng/m^3 for the Sea of Japan and 1.46 ng/m^3 for the East China Sea.

The temporal distribution of Hg(0) in the surface atmosphere during the investigated period is not homogeneous (Fig. 2). The median concentrations in October 2019 were 1.23 ng/m^3 for the Sea of Japan and 1.05 ng/m^3 for the East China Sea. In December 2019, median concentrations of 1.26 ng/m^3 were obtained for the Sea of Japan and 1.46 ng/m^3 for the East China Sea. Between October and December, some meteorological parameters decrease:

- Average temperature from 15.2 to 8.5 °C;
- Humidity from 69 to 62 %;
- Solar radiation from 140 to 91 W/m^2/h.

Two main regions with elevated mercury emissions are identified by the CWT analysis. These are Eastern China and the Korean Peninsula (Fig. 3). With a resolution of the grid cell size (i, j): 1 × 1°, the southern part of the Sea of Japan can be considered as a potential source (Fig. 3a). A detailed investigation reveals that the elevated concentrations in this area are due to the arrival of two air masses from northern and northeastern China by different routes. One is through the Korean Peninsula and the other through the central Sea of Japan. This is evident with the high resolution of 0.1 × 0.1° CWT analysis. (Fig. 3c).

The distribution of CWT within the regions is quite varied (Fig. 4). In order to assess the reliability of the analysis, data on the percentage coverage of the region and the number of points on the CWT trajectory are presented (Table 2). For Northeastern China, South-central China, and Russia, the coverage does not exceed 15 % of the total territory, indicating a weak reliability of this analysis for these areas. Among regions with a coverage percentage greater than 60 %, higher CWT values were observed over the eastern Chinese and South Korean territories (1.49 and 1.45 ng/m^3). It should be noted that all the seas have similar median CWT values (between 1.22 and 1.24 ng/m^3), except for the Korean Gulf, which has a slightly higher value (1.35 ng/m^3).

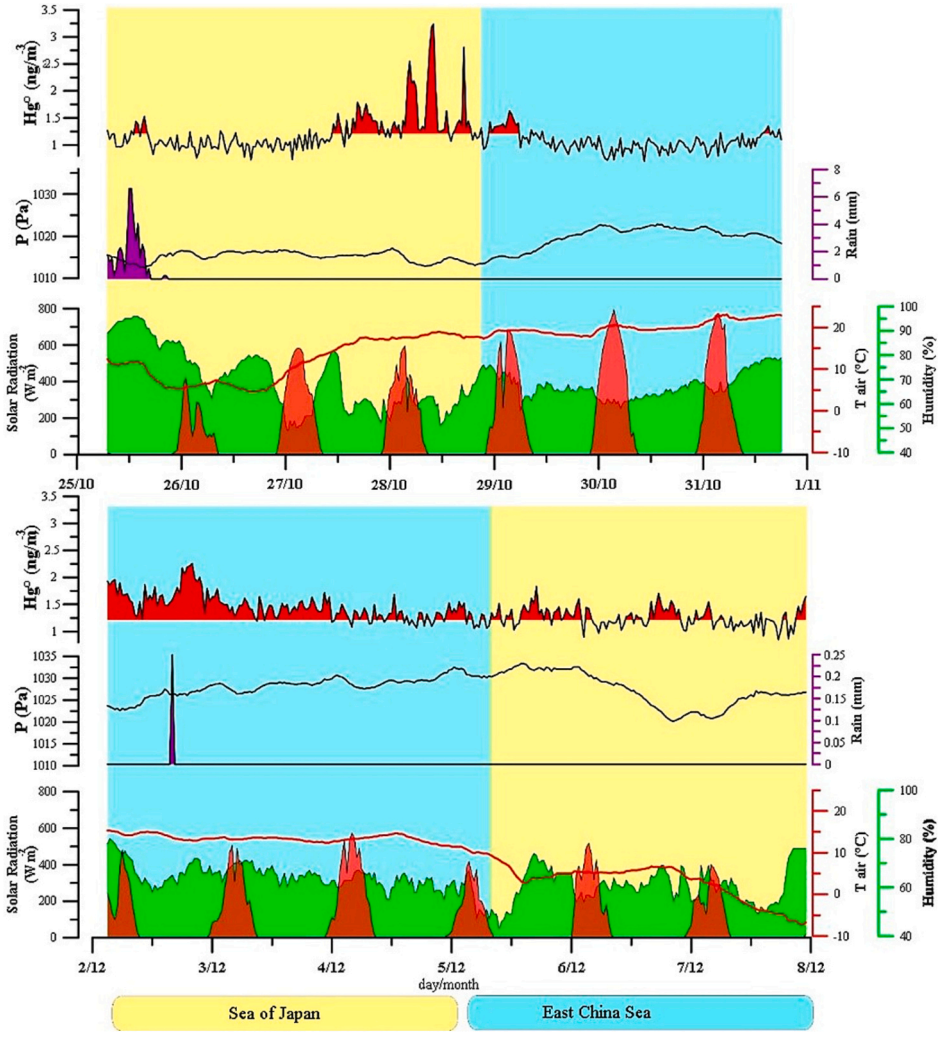

Fig. 2. Temporal distribution of Hg(0) and some meteorological parameters in the surface atmosphere during the 88th voyage of the Academic Lavrentyev R/V, autumn-winter 2019.
Source: Compiled by the authors.

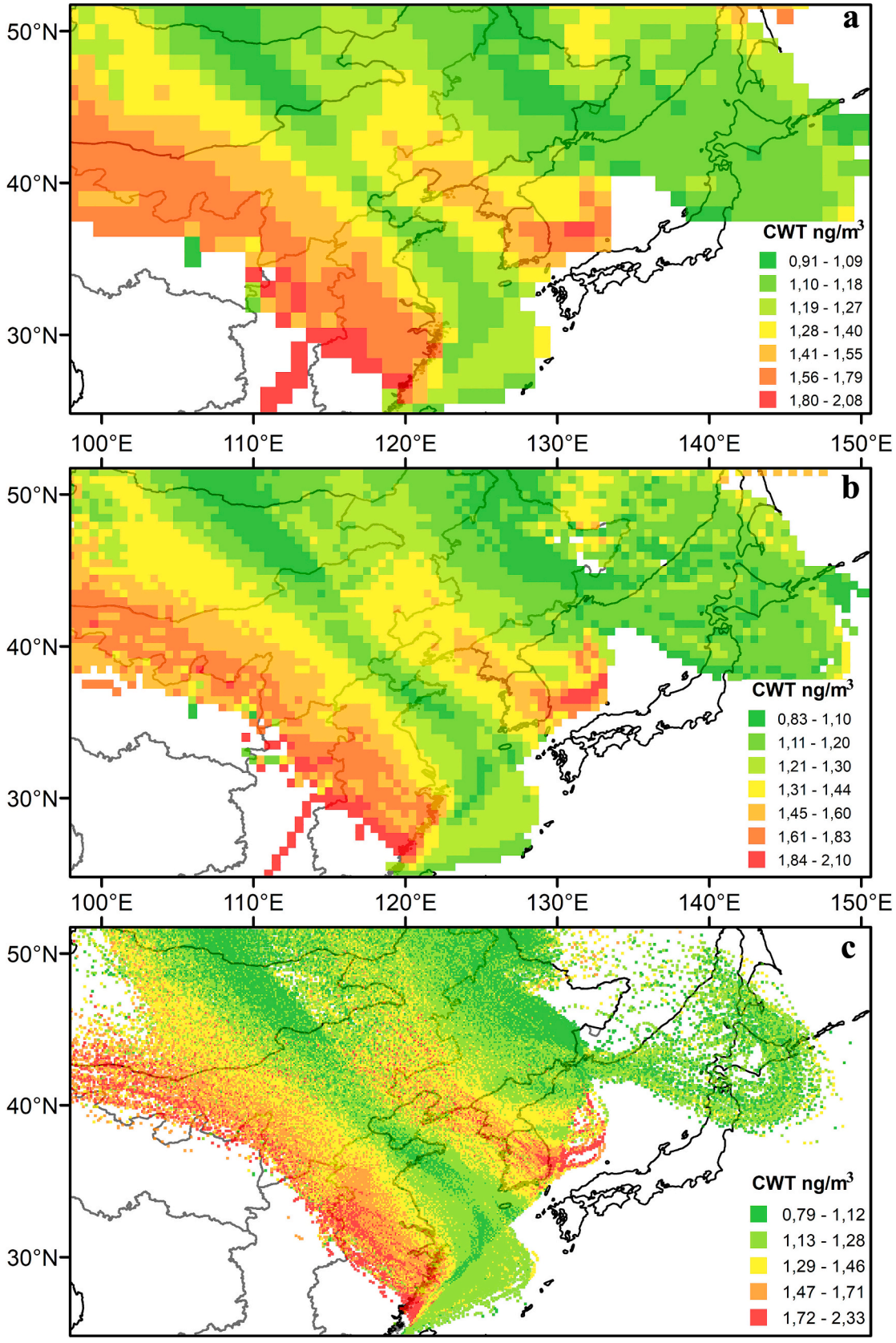

Fig. 3. Results of the CWT analysis at different resolutions a – 1 × 1°, b – 0.5 × 0.5, c– 0.1 × 0.1° for the investigated period.
Source: Compiled by the authors.

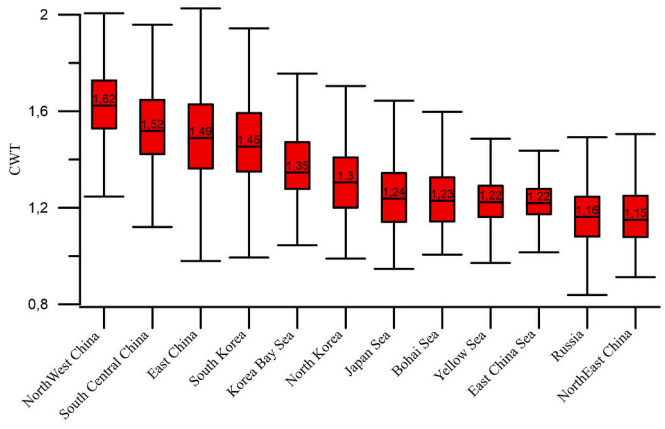

Fig. 4. Distribution of CWT Values by Region.
Source: Compiled by the authors.

The determined average concentration of Hg(0) in the surface atmosphere of the Sea of Japan in October 2019 is 1.23 ng/m^3. It is significantly lower than the previously reported concentration of 1.8 ng/m^3 in October 2010 (Kalinchuk and Astakhov, 2014) and 1.39 ng/m^3 in October 2018 (Kalinchuk et al., 2020). For the East China Sea, the average values obtained in October 2019 are 1.05 ng/m^3. It is half the value previously recorded in October–November 2013, when they amounted to 2.2 ng/m^3 (Wang et al., 2016a). The median concentrations of atomic mercury obtained during the investigated period are significantly lower than the average for the Northern Hemisphere of 1.5–1.7 ng/m^3 (Lindberg et al., 2007). It can be attributed to the global tendency for Hg(0) concentration to decrease in the surface atmosphere (Zhang et al., 2016). In more detail, all the measurements are presented in Table 1.

The obtained data of Hg(0) in the surface atmosphere in the East China Sea for December 2019 is 1.46 ng/m^3, which is significantly higher than in October, which is 1.05 ng/m^3. The increased concentrations in the surface atmosphere of the Sea of Japan and the East China Sea in winter compared to autumn are probably due to the increased anthropogenic impact on the air masses, such as the beginning of the heating season and the burning of biomass (Liu et al., 2019a).

The increase in analysis resolution to 0.1 × 0.1° made it possible to localize the source regions. On the Korean peninsula, the southeastern part is highlighted. According to data (AMAP/UNEP, 2013; Zhang et al., 2015), there are no major sources of mercury in this region. However, it was previously found that the transboundary transport of Hg(0) from northern regions of China greatly affects the region (Liu et al., 2019b). The presented data from CWT analysis coincide with the PSCF (potential source contribution method) describing the transfer of Hg(0) from northern and eastern China (Liu et al., 2019b).

In the territorial comparison of CWT, East China's leadership can be attributed to its global dominance in mercury emissions(AMAP/UNEP, 2013). The increased value of CWT over the territory of the Korean Gulf is associated with previously repeatedly recorded transfers of Hg(0) from the northern regions of China to the Korean Peninsula (Nguyen et al., 2011).

The reported data on Hg(0) concentration in the surface atmosphere complements the global data during the autumn and winter periods. The measures were first taken in December for the East China Sea. The obtained mercury concentrations reveal the global tendency towards lower concentrations of atomic mercury in the atmosphere and increased

Table 1
Data on the content of Hg(0) in the surface atmosphere of the East Asian seas.

Region	Time	Device	Min. — max.	Mean	Median	SD	Published
Japan Sea	October 2019	RA—915M	0.72—3.23	1.23	1.14	0.39	In this work
	December 2019	RA—915M	0.85—1.83	1.26	1.25	0.17	In this work
	December 2018	RA—915M	0.60—2.48	1.19	1.19	0.16	(Lopatnikov and Kalinchuk, 2019)
	February 1990		0.64—0.79	0.7		0.08	(Stepanov and Kalyagin, 1997)
	July 2007	RA—915+	0.50— 9.8	2.8		NA	(Astakhov et al., 2011a) (Astakhov et al., 2011b)
	July–August 2008	Tekran 2537B	0.30—1.59	0.8		0.36	(Kang and Zhouqing, 2011)
	September 2008	Tekran 2537B	0.70—2.24	1.14		0.23	(Kang and Zhouqing, 2011)
	November 2010	RA—915+	0.60—3.80	1.9		0.8	(Aksentov, 2012)
	October 2010	RA—915+	0.70—2.80	1.8	1.7	0.4	(Kalinchuk and Astakhov, 2014)
	September–October 2015	RA—915M	0.30—5.20	1.6	1.6	0.6	(Kalinchuk et al., 2018)
	September 2018	RA—915M	1.15—2.50	1.59	1.51	0.22	(Kalinchuk et al., 2020)
	October 2018	RA—915M	1.23—1.55	1.39	1.39	0.07	(Kalinchuk et al., 2020)
	August–September 2017	RA—915+	1.09—2.41	1.62	1.61	0.18	(Kalinchuk et al., 2019)
Bohai Sea	May 2012	Tekran 2537B		2.71		0.49	(Wang et al., 2020)
	November 2012	Tekran 2537B		1.98		0.91	(Wang et al., 2020)
	May 2014	Tekran 2537B		2.51		0.77	(Wang et al., 2020)
	November 2014	Tekran 2537B		3.64		2.54	(Wang et al., 2020)
Bohai Sea and Yellow Sea	April–May 2014	Tekran 2537B		2.03		0.72	(Wang et al., 2016b)
	November 2014	Tekran 2537B		2.09		1.58	(Wang et al., 2016b)
	November 2013	Gold trap	0.2–9.2	2.1		1.1	(Wang et al., 2017)
Yellow Sea	May 2014	Tekran 2537B		1.89		0.4	(Wang et al., 2020)
	November 2014	Tekran 2537B		1.59		0.5	(Wang et al., 2020)
	May 2012	RA—915+	0.85—2.79	1.86		0.40	(Ci et al., 2015)
	November 2012	RA—915+	0.93—5.09	1.84		0.50	(Ci et al., 2015)
	July 2010	RA—915+	1.68—4.34	2.61		0.50	(Ci et al., 2011)
	September 2007	RA—915+	1.56—2.97	2.43	2.28	0.59	(Nguyen et al., 2011)
	October 2007	RA—915+	1.29—2.36	1.82	1.81	0.51	(Nguyen et al., 2011)
	April 2008	RA—915+	1.36—1.99	2.03	1.86	0.66	(Nguyen et al., 2011)
East China Sea	June–July 2013	Tekran 2537B		1.61			(Wang et al., 2016a)
	October–November 2013	Tekran 2537B		2.20			(Wang et al., 2016a)
	October 2019	RA—915M	0.7–1.63	1.05	1.04	0.17	In this work
	Декабрь 2019	RA—915M	1.05–2.26	1.46	1.41	0.25	In this work
East China Sea and South China Sea	October 1989		0.90—20.8	8.31		5.76	(Stepanov and Kalyagin, 1997)

Source: Compiled by the authors.

Table 2
The CWT value, the number of points and the % coverage of the region.

Region	CWT	The number of trajectory points in region (i, j)	The coverage of the region is % of its territory.
NortEast China	1,15	70,193	87,7
Russia	1,16	50,342	14,4
East China Sea	1,22	68,321	62,6
Yellow Sea	1,22	69,883	100
Bohai Sea	1,23	8977	100
Japan Sea	1,23	31,331	50,9
Nort China	1,28	90,430	91,4
North Korea	1,30	17,831	100
Korea Bay Sea	1,35	8289	100
South Korea	1,45	15,490	100
East China	1,49	61,346	67,2
South Central China	1,52	4158	13,5
NortWest China	1,62	1122	12

Source: Compiled by the authors.

emissions during the winter period due to the beginning of the heating season.

The application of the CWT analysis with high resolution enabled us to detect emissions and analysis mistakes without the need to increase the number of trajectory intersections in the grid cell as previously required (Kalinchuk et al., 2020). The increased resolution makes it possible to see zones of atomic mercury transport and to localize sources beyond the region but within parts of the region, even considering the short period of the research.

The peculiarity of the vessel's movement made it possible to investigate regions both close to sources of anthropogenic mercury emissions and vulnerable to their influence. The identification of discharge zones through the high resolution CWT analysis will make it possible to define the boundaries of such zones and the sources influencing them in longer studies. By employing the geoprocessing technique for regional comparison of CWT data, we can clearly assess the relative contribution of each area.

CRediT authorship contribution statement

E.A. Lopatnikov: Writing – original draft, Visualization, Validation, Methodology, Data curation, Conceptualization. **M.V. Ivanov:** Writing – review & editing, Formal analysis, Data curation.

Declaration of competing interest

The authors declare that they have no known competing financial interests or personal relationships that could have appeared to influence the work reported in this paper.

Acknowledgements

The authors would like to express their gratitude to Dr. A.S. Astakhov for his valuable comments and suggestions that greatly improved the manuscript. We also want to thank Dr. R.B. Shakirov for organizing and managing the cruises. This work was supported by the Ministry of Science and Higher Education of the Russian Federation (124022100084-8, 124022100076-3). The author gratefully acknowledges the NOAA Air Resources Laboratory (ARL) for the provision of the HYSPLIT transport and dispersion model and READY website (http://www.ready.noaa.gov) used in this publication.

Data availability

Data will be made available on request.

References

AMAP/UNEP, 2013. Technical background report for the global mercury assessment 2013., in: Norway/UNEP ChemicalsBranch (Ed.), Arctic Monitoring and Assessment Programme. Geneva, Oslo, p. 263.

Aksentov, K.I., Kalinchuk, V.V., 2012. Atomic Mercury Distribution Features in the Surface Air Layer in the Sea of Japan in the Fall of 2010. Russ. Meteorol. Hydrol. 37 (10), 674–680. https://doi.org/10.3103/S1068373912100056.

Astakhov, A.S., Aksentov, K.I., Belous, O.V., Gulenko, T.A., Zhukovin, A.Yu., Karnaukh, V.N., Yanovskaya, O.S., 2011a. Geological and Geoecological Research in the Sea of Japan in Cruise 45 of the R/V 'Professor Gagarinskiy' (October-November 2009) [in Russian]. Russ. J. Pac. Geol. 30 (1), 119–124.

Astakhov, A.S., Ivanov, M.V., L, B.Ya., 2011b. Hydrochemical and Atmochemical Mercury Dispersion Zones over Hydrothermal Vents of the Submarine Piip Volcano in the Bering Sea. Oceanology 51 (5), 826–835. https://doi.org/10.1134/S0001437011050031.

Beckers, F., Rinklebe, J., 2017. Cycling of mercury in the environment: sources, fate, and human health implications: a review. Crit. Rev. Environ. Sci. Technol. 47, 693–794. https://doi.org/10.1080/10643389.2017.1326277.

CASM, C.A. of S. and M, Washington, C. in T, S.-C.-U. of, CIESIN, C. for I.E.S.I.N, 1996. China Dimensions Data Collection: China Administrative Regions GIS Data: 1:1M, County Level (1 July 1990).

Chen, L., Liang, S., Liu, M., Yi, Y., Mi, Z., Zhang, Y., Li, Y., Qi, J., Meng, J., Tang, X., Zhang, H., Tong, Y., Zhang, W., Wang, X., Shu, J., Yang, Z., 2019. Trans-provincial health impacts of atmospheric mercury emissions in China. Nat. Commun. 10, 1–12. https://doi.org/10.1038/s41467-019-09080-6.

Ci, Z.J., Zhang, Xiaoshan, Wang, Z.W., Niu, Z.C., Diao, X.Y., Wang, S.W., 2011. Distribution and Air-Sea Exchange of Mercury (Hg) in the Yellow Sea. Atmospheric Chem. Phys. 11 (6), 2881–2892. https://doi.org/10.5194/acp-11-2881-2011.

Ci, Z., Wang, C., Wang, Z.W., Zhang, X., 2015. Elemental Mercury (Hg(0)) in Air and Surface Waters of the Yellow Sea during Late Spring and Late Fall 2012: Concentration, Spatial-Temporal Distribution and Air/Sea Flux. Chemosphere 119, 199–208. https://doi.org/10.1016/j.chemosphere.2014.05.064.

Fang, X., Saito, T., Park, S., Li, S., Yokouchi, Y., Prinn, R.G., 2018. Performance of Back-trajectory statistical methods and inverse modeling method in locating emission sources. ACS Earth Sp. Chem. 2, 843–851. https://doi.org/10.1021/acsearthspacechem.8b00062.

Fu, X.W., Feng, X.B., Shang, L.H., Wang, S.F., Zhang, H., 2012. Two years of measurements of atmospheric total gaseous mercury (TGM) at a remote site in Mt. Changbai area. Northeastern China. Atmos. Chem. Phys. 12, 4215–4226. https://doi.org/10.5194/acp-12-4215-2012.

Gustin, M.S., Amos, H.M., Huang, J., Miller, M.B., Heidecorn, K., 2015. Measuring and Modeling Mercury in the Atmosphere : A Critical Review 5697–5713. https://doi.org/10.5194/acp-15-5697-2015.

Kalinchuk, V., Yatsuk, A., Marchesini, L.B., Lopatnikov, E., Nesterova, O., Valentini, R., Aksentov, K., 2022. The first simultaneous and continuous underway measurements of atmospheric gaseous elemental mercury, carbon dioxide and methane in the marine boundary layer: results of cruise study in the sea of Japan in may 2018. Atmos. Pollut. Res. 13, 101458. https://doi.org/10.1016/j.apr.2022.101458.

Kalinchuk, V.V., 2023. Gaseous elemental mercury and its evasion fluxes in the marine boundary layer of the marginal seas of the northwestern Pacific: results from two cruises in September–December 2019. Sci. Total Environ. 858, 159711. https://doi.org/10.1016/j.scitotenv.2022.159711.

Kalinchuk, V.V., Aksentov, K.I., Karnaukh, V.N., 2019. Gaseous Elemental Mercury (Hg (0)) in the Surface Air over the Sea of Japan, the Sea of Okhotsk and the Kuril-Kamchatka Sector of the Pacific Ocean in August–September 2017. Chemosphere 224, 668–679. https://doi.org/10.1016/j.chemosphere.2019.02.185.

Kalinchuk, V.V., Astakhov, A.S., 2014. Atmochemical mercury dispersion aureoles over active geologic structures of the northern sea of Japan. Russ. Geol. Geophys. 55, 1379–1386. https://doi.org/10.1016/j.rgg.2014.11.002.

Kalinchuk, V.V., Lopatnikov, E.A., Astakhov, A.S., 2018. Gradient measurements of gaseous elemental mercury (Hg0) in the marine boundary layer of the northwest sea of Japan (East Sea). Environ. Pollut. 237, 1124–1136. https://doi.org/10.1016/j.envpol.2017.11.055.

Kalinchuk, V.V., Lopatnikov, E.A., Astakhov, A.S., Ivanov, M.V., Hu, L., 2020. Distribution of atmospheric gaseous elemental mercury (Hg (0)) from the Sea of Japan to the Arctic , and Hg (0) evasion fluxes in the Eastern Arctic Seas. Sci. Total Environ. 753, 142003. doi:https://doi.org/10.1016/j.scitotenv.2020.142003.

Kang, H., Zhouqing, X., 2011. Atmospheric Mercury over the Marine Boundary Layer Observed during the Third China Arctic Research Expedition. J. Environ. Sci. 23 (9), 1424–1430. https://doi.org/10.1016/S1001-0742(10)60602-X.

Lindberg, S., Bullock, R., Ebinghaus, R., Engstrom, D., Feng, X.B., Fitzgerald, W., Pirrone, N., Prestbo, E., Seigneur, C., 2007. A synthesis of progress and uncertainties in attributing the sources of mercury in deposition. Ambio 36, 19–32. https://doi.org/10.1579/0044-7447(2007)36[19:ASOPAU]2.0.CO;2.

Liu, C., Fu, X.W., Zhang, H., Ming, L., Xu, H., Zhang, L., Feng, X.B., 2019b. Sources and outflows of atmospheric mercury at Mt. Changbai, northeastern China. Sci. Total Environ. 663, 275–284. https://doi.org/10.1016/j.scitotenv.2019.01.332.

Liu, Chen, Fu, X.W., Zhang, H., Ming, L., Xu, H., Zhang, L., Feng, X.B., 2019a. Sources and outflows of atmospheric mercury at Mt. Changbai, northeastern China. Sci. Total Environ. 663, 275–284. https://doi.org/10.1016/j.scitotenv.2019.01.332.

Lopatnikov, E.A., Kalinchuk, V.V., 2019. Gaseous elemental mercury (Hg(O)) in the surface atmosphere and Hg(O) fluxes from the sea surface to the atmosphere in the Sea of Japan in December 2018. In: I.O., RAS (Ed.), Geology of Seas and Oceans: Proceedings of XXIII International Conference on Marine Geology, pp. 269–272. https://doi.org/10.29006/978-5-9901449-8-9.ICMG-2019-4. Moscow.

Nguyen, D.L., Kim, J.Y., Shim, S.G., Zhang, X., 2011. Ground and shipboard measurements of atmospheric gaseous elemental mercury over the Yellow Sea region during 2007-2008. Atmos. Environ. 45, 253–260. https://doi.org/10.1016/j.atmosenv.2010.07.021.

Pirrone, N., Cinnirella, S., Feng, X., Finkelman, R.B., Friedli, H.R., Leaner, J., Mason, R., Mukherjee, A.B., Stracher, G.B., Streets, D.G., Telmer, K., 2010. Global mercury emissions to the atmosphere from anthropogenic and natural sources. Atmos. Chem. Phys. 10, 5951–5964. https://doi.org/10.5194/acp-10-5951-2010.

Sholupov, S., Pogarev, S., Ryzhov, V., Mashyanov, N., Stroganov, A., 2004. Zeeman atomic absorption spectrometer RA-915+ for direct determination of mercury in air and complex matrix samples. Fuel Process. Technol. 85, 473–485. https://doi.org/10.1016/j.fuproc.2003.11.003.

Stepanov, I.I., Kalyagin, A.N., 1997. Distribution of mercury concentration in the atmosphere over the Western Pacific [in Russian]. Bull. Far East Branch RAS 3, 48e56.

UNEP, U, 2013. Global Mercury Assessment 2013: Sources, Emissions. Releases and Environmental Transport. UNEP Chem, Branch, Geneva, Switz.

Wang, C., Zhijia Ci, Wang, Z.W., 2016a. Air-sea exchange of gaseous mercury in the East China Sea. Environ. Pollut. 212, 535–543. https://doi.org/10.1016/j.envpol.2016.03.016.

Wang, C., Ci, Z., Wang, Z.W., Zhang, X., Jia, G., 2016b. Speciated Atmospheric Mercury in the Marine Boundary Layer of the Bohai Sea and Yellow Sea. Atmospheric Environ. 131, 360–370. https://doi.org/10.1016/j.atmosenv.2016.02.021.

Wang, Q., Shen, W., Ma, Z., 2000. Estimation of mercury emission from coal combustion in China. Environ. Sci. Technol. 34, 2711–2713. https://doi.org/10.1021/es990774j.

Wang, Y., Liu, R., Li, Y., Cui, X., Zhou, J., Liu, S., Zhang, Y., 2017. GEM in the marine atmosphere and air-sea exchange of hg during late autumn and winter cruise campaigns over the marginal seas of China. Atmos. Res. 191, 84–93. https://doi.org/10.1016/j.atmosres.2017.03.004.

Wang, C., Wang, Z.W., Zhang, X., 2020. Characteristics of Mercury Speciation in Seawater and Emission Flux of Gaseous Mercury in the Bohai Sea and Yellow Sea. Environ. Res. 182 (2019), 109092. https://doi.org/10.1016/j.envres.2019.109092.

Zhang, H., Fu, X.W., Lin, C.J., Wang, X., Feng, X.B., 2015. Observation and analysis of speciated atmospheric mercury in Shangri-La, Tibetan plateau. China. Atmos. Chem. Phys. 15, 653–665. https://doi.org/10.5194/acp-15-653-2015.

Zhang, Y., Jacob, D.J., Horowitz, H.M., Chen, L., Amos, H.M., Krabbenhoft, D.P., Slemr, F., St. Louis, V.L., Sunderland, E., 2016. Observed decrease in atmospheric mercury explained by global decline in anthropogenic emissions. Proc. Natl. Acad. Sci. U. S. A. 113, 526–531. doi:https://doi.org/10.1073/pnas.1516312113.